2-3-2. Three-terminal tandem solar cell

From formula (2-23), it can be seen that the minority-carrier diffusion length ($L_n$) of GaAs-on-Si is not only affected by the concentration $N_A$ but also by the dislocation density $N_d$. This property was described in Fig. 2-4 with a 3-dimensional graph. Considering formula (2-24), $L_p$ has a property similar to $L_n$.

Fig. 2-5 shows the effect of dislocation density on the spectral response of the GaAs top cell on Si. When $N_d > 10^6$ $cm^{-2}$, there is a serious effect on the GaAs top cell. It degrades the quantum efficiency in whole wavelength region.

Fig. 2-6 shows calculated efficiency, open-circuit voltage and short-circuit current for the GaAs top cell as a function of the dislocation density. The dislocations act as recombination centers in the active layers of the GaAs cell on Si, which shorten the minority-carrier lifetimes and result in decrease of *Jsc*. On other way, the dark-saturation current is also increased by the dislocations [85] and it make Voc reduced. So the conversion efficiency of the GaAs top cell on Si decreases rapidly with increase of the dislocations. From these results, it can be found that if the dislocation density can be reduced to less than $8 \times 10^5$ $cm^{-2}$, the calculated efficiency will be boosted more than 20%.

Fig. 2-7 shows effect of the carrier concentration of n-GaAs base layer on the spectral response of the GaAs top cell on Si. The spectral response is enhanced in the long wavelength region by reducing the concentration of n-GaAs base layer. Voc is increased with increase of the concentration,

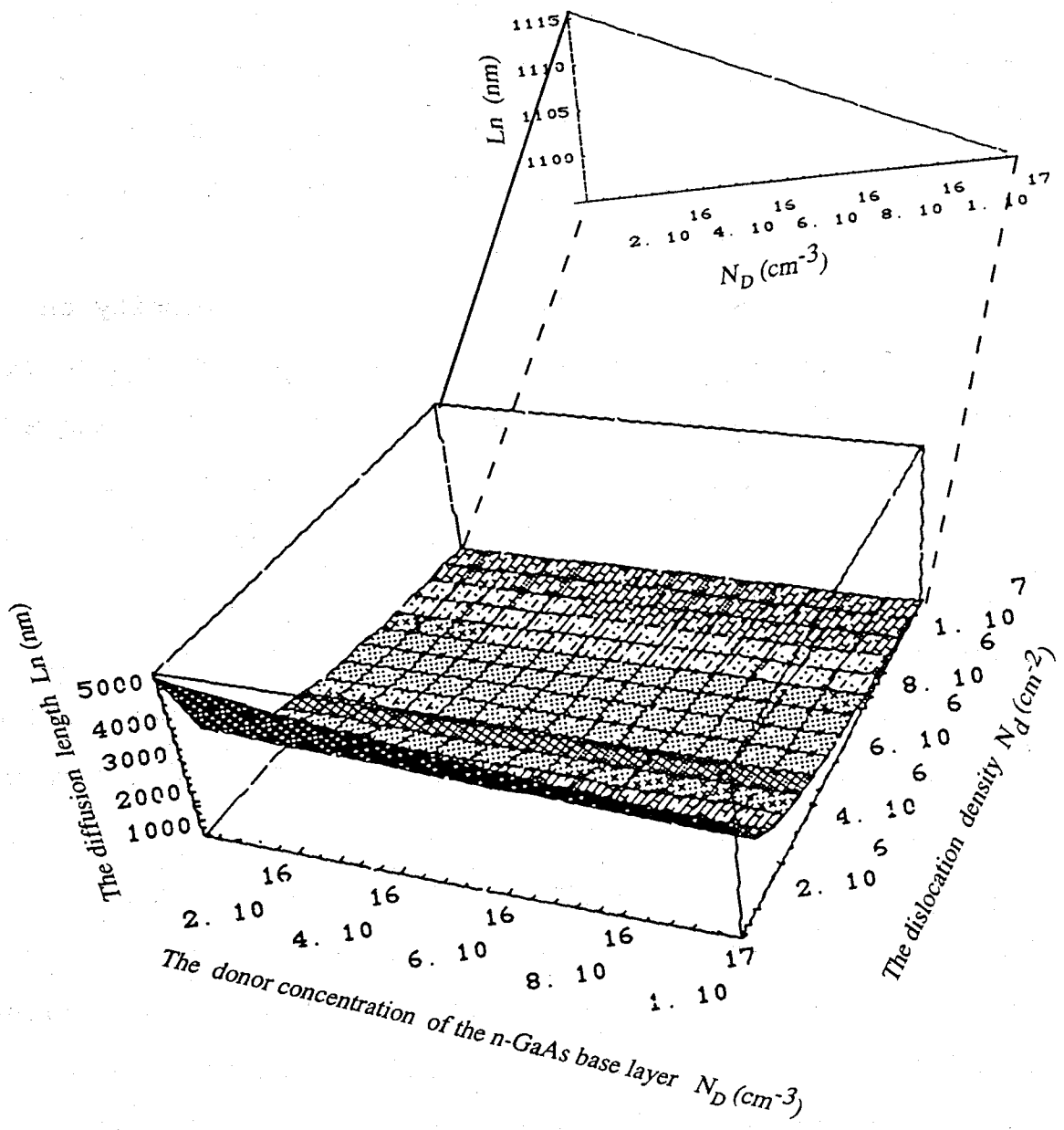


**Fig.2-4 The relationship of the diffusion length *Ln* vs. the dislocation density and the donor concentration.**

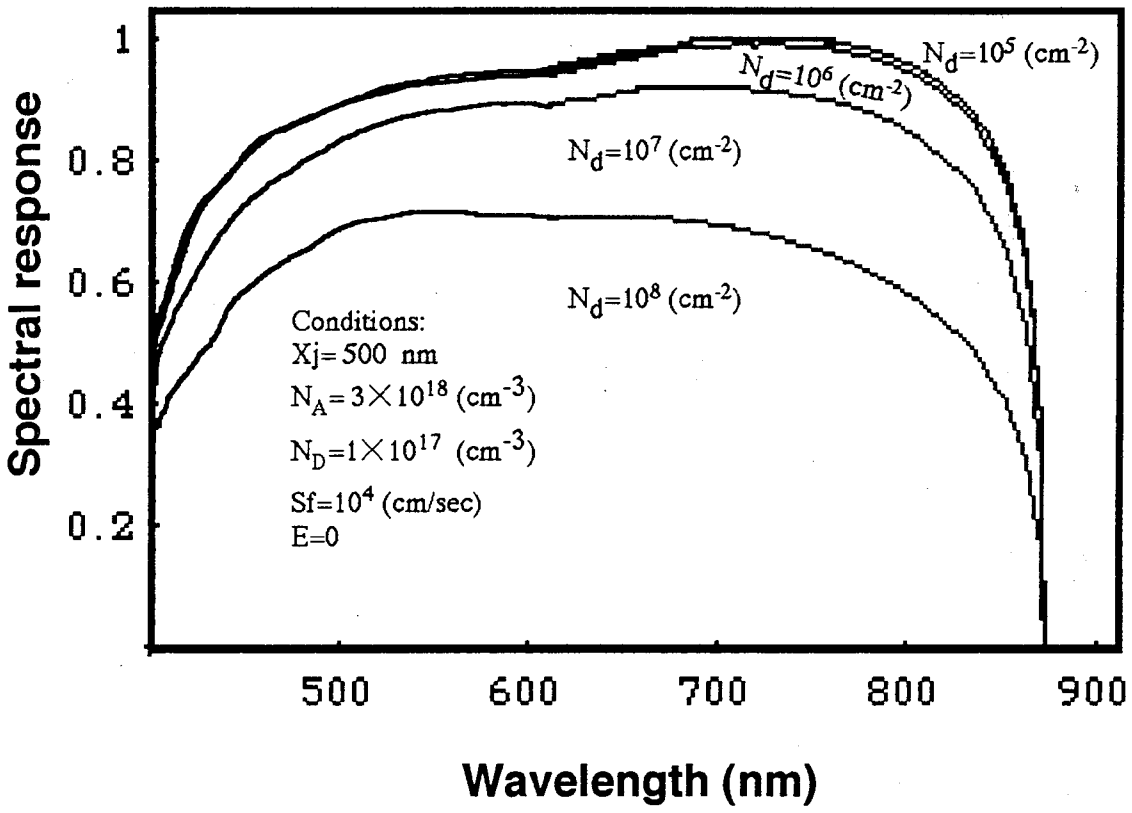


**Fig.2-5 The effects of the dislocation density on the spectral response of the GaAs top cell on Si.**

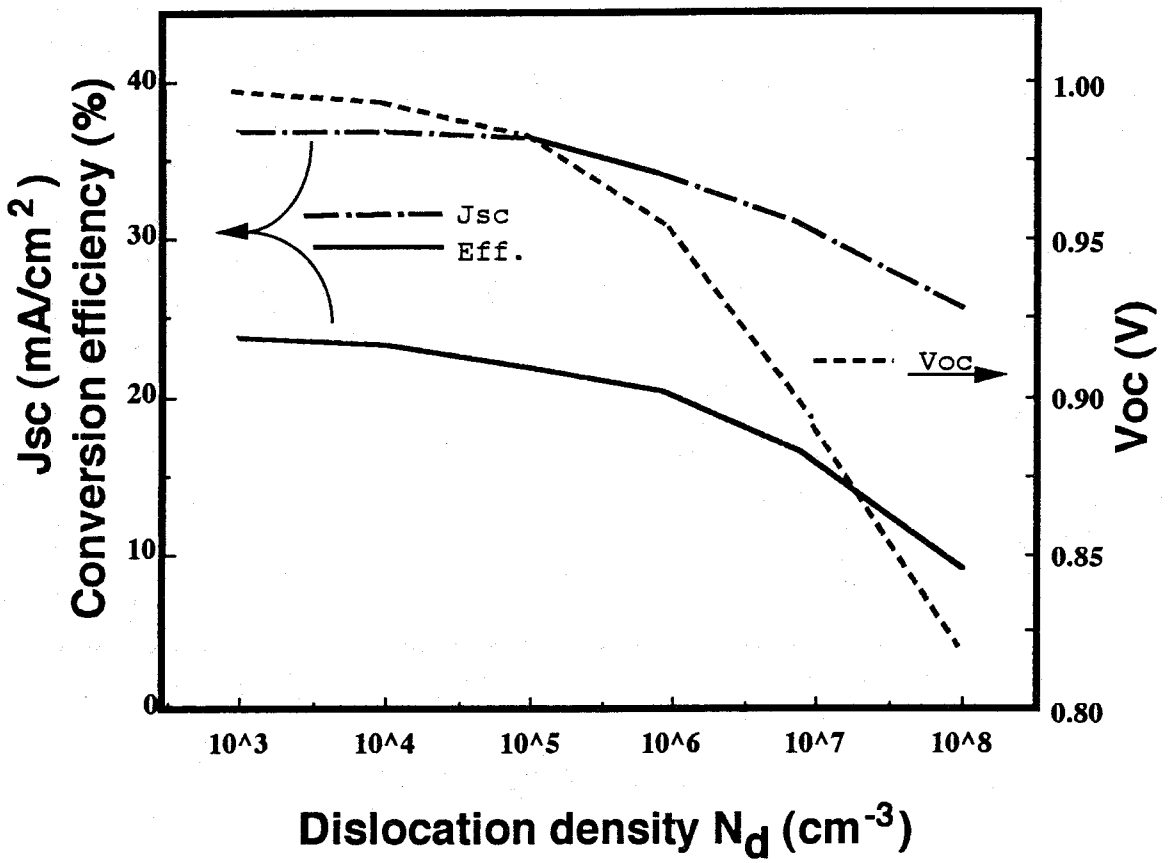


Fig. 2-6 The effects of dislocation density Nd on the characteristics of the GaAs top cell on Si ( under conditions: $S_f=10^4$ cm/sec, $N_A=3\times10^{18}$ $cm^{-3}$, $N_D=1\times10^{17}$ $cm^{-3}$, $X_j=500$ nm, E=0).

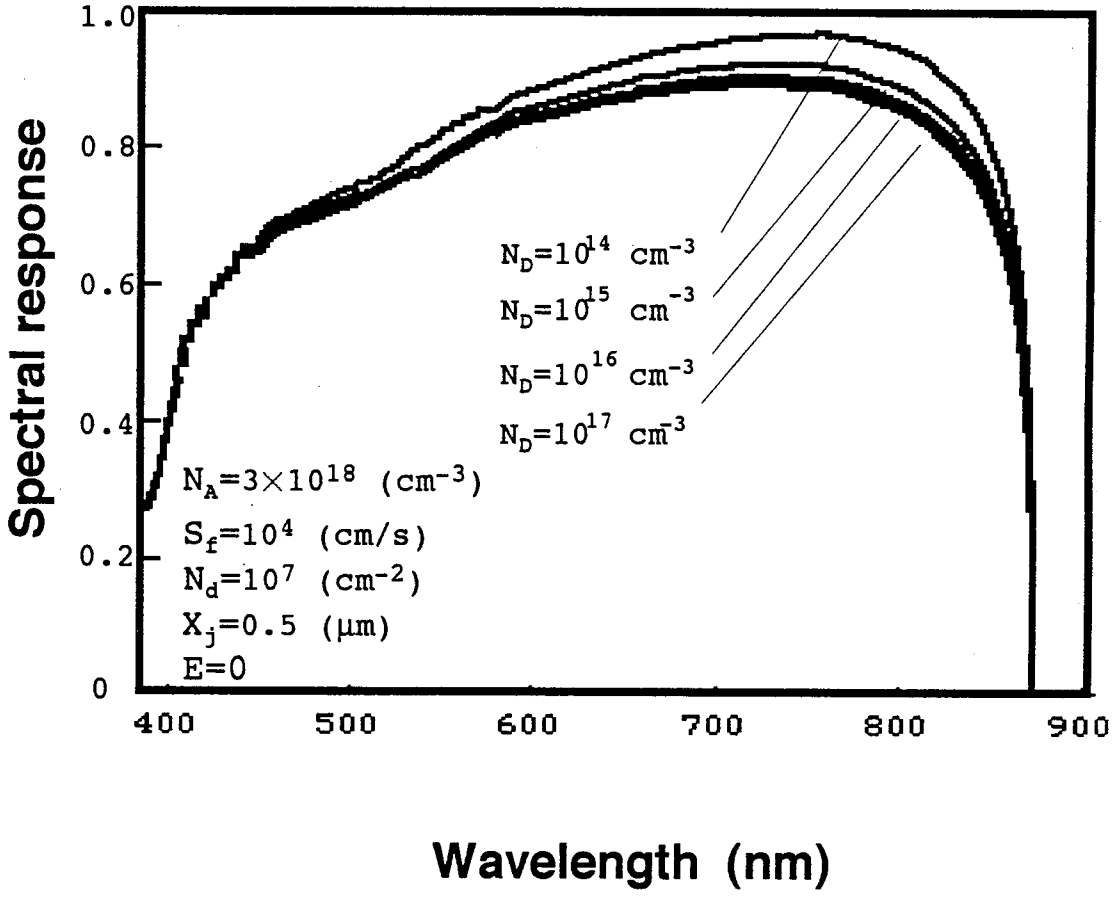


**Fig.2-7 The effect of carrier concentration of the n-GaAs base layer on the spectral response of the GaAs top cell on Si.**

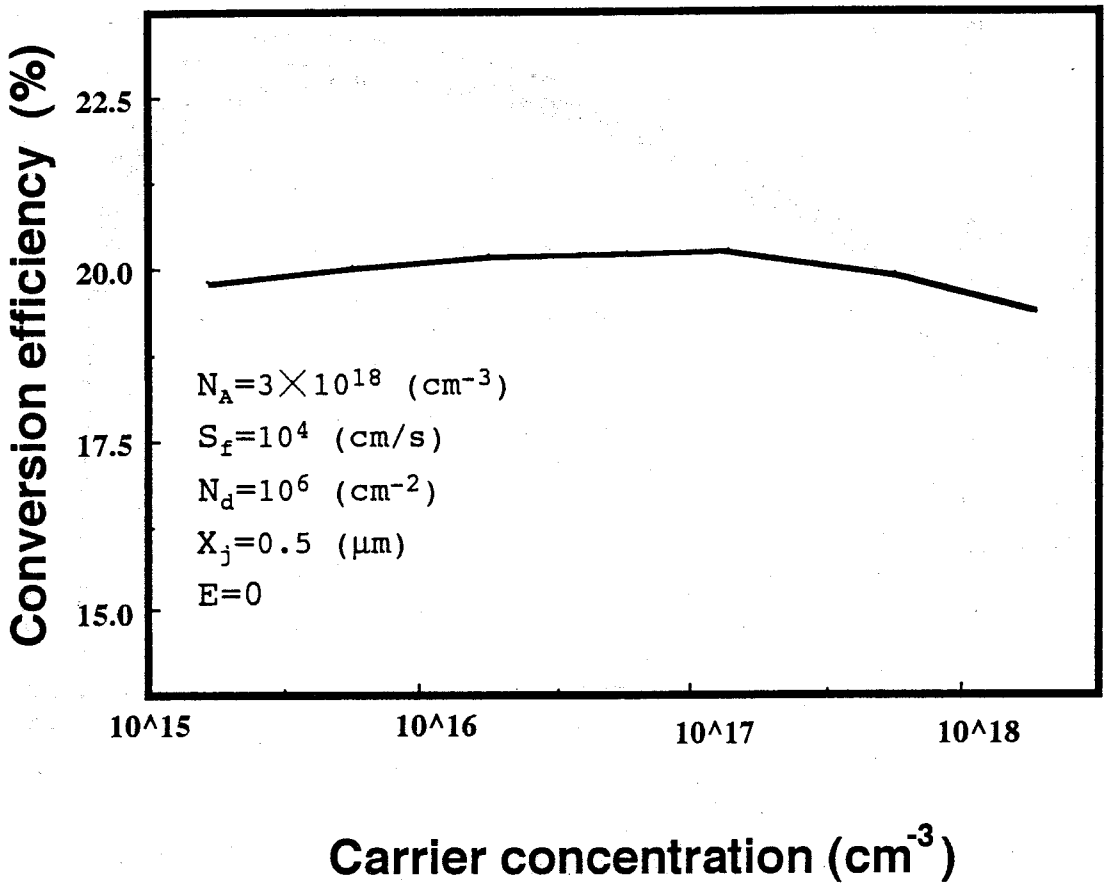


**Fig.2-8 The effect of the carrier concentration of n-GaAs base layer on the conversion efficiency of the GaAs top cell on Si.**

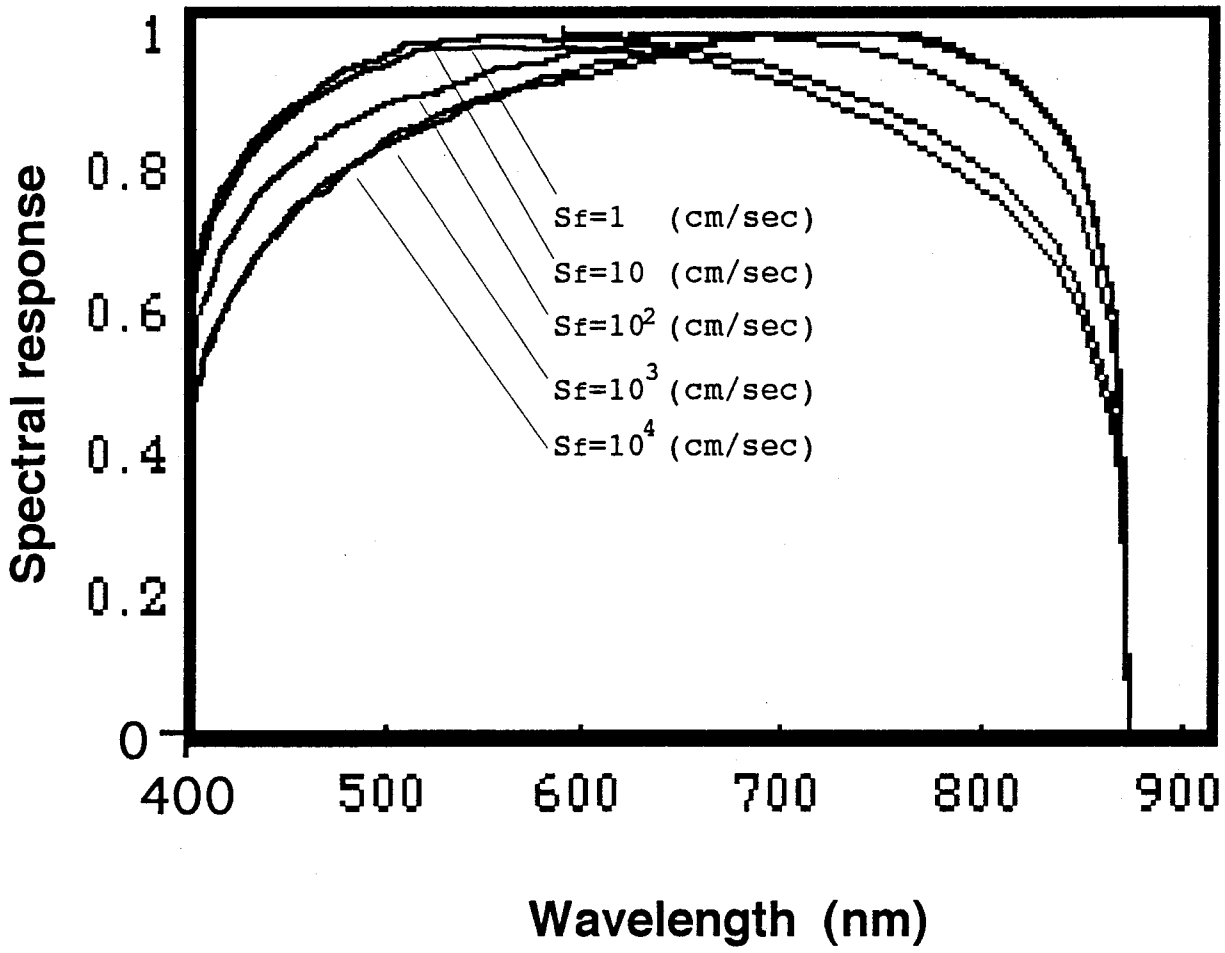


Fig.2-9 Calculated spectral response of the GaAs top cell on Si as a function of the front surface recombination velocities $S_f$ ( under condition: $N_A=3\times10^{18}$ cm$^{-3}$, $N_D=1\times10^{17}$ cm$^{-3}$, $X_j=500$ nm, $N_d=10^6$ cm$^{-2}$, E=0).

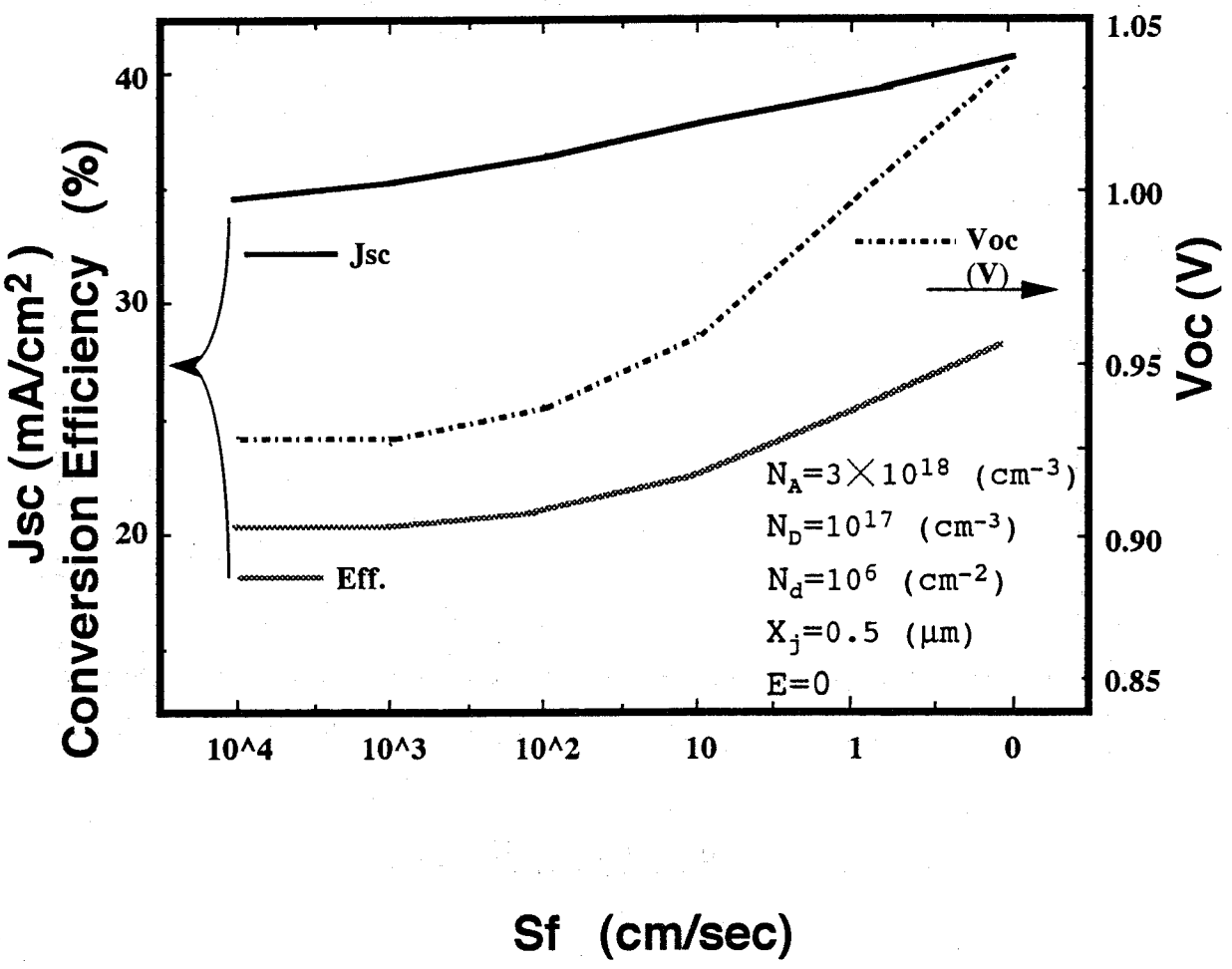


Fig.2-10 Dependence of photovoltaic characteristics of the GaAs top cell on the front surface recombination velocity $S_f$.

but Jsc is decreased simultaneously. The optimal concentration for the efficiency is about $1\times10^{17}$ $cm^{-3}$. That is shown in Fig. 2-8.

Fig. 2-9 shows calculated spectral response of the GaAs top cell on Si as a function of the front surface recombination velocity ($S_f$). The spectral response in the wavelength region from 400 to 650 nm is relatively enhanced by decreasing $S_f$. The dependence of the photovoltaic characteristics of the GaAs top cell on Si is shown in Fig. 2-10. For ideal condition, $S_f=0$, the calculated AM0 efficiency will approach to 27%.

The spectral response of the GaAs top cell is contributed by the p-GaAs emitter layer and the n-GaAs base layer in the most part, because the contribution of the depletion layer is small enough to neglect in comparison with them. From the numerical analysis, it was found that there is a critical junction depth ($X_j$) about 400 nm. Fig. 2-11 (a) shows when $X_j=300$ nm, the contribution fraction of the n-GaAs base layer to the spectral response is larger than the p-GaAs emitter layer. However, when $X_j$ = 500 nm reversely, the contribution fraction of n-GaAs base layer is smaller than p-GaAs emitter layer. That is shown in Fig 2-11 (b).

Using a graded bandgap emitter layer (GBEL) for the GaAs top cell, it provides an electric field in the emitter region. The effective electron diffusion length ($L_{nn}$) can be expressed as formula (2-35). $L_{nn}$ is a function of the electric field strength (E) and the dislocation density. These properties are described in Fig. 2-12. Fig. 2-13 demonstrates the spectral

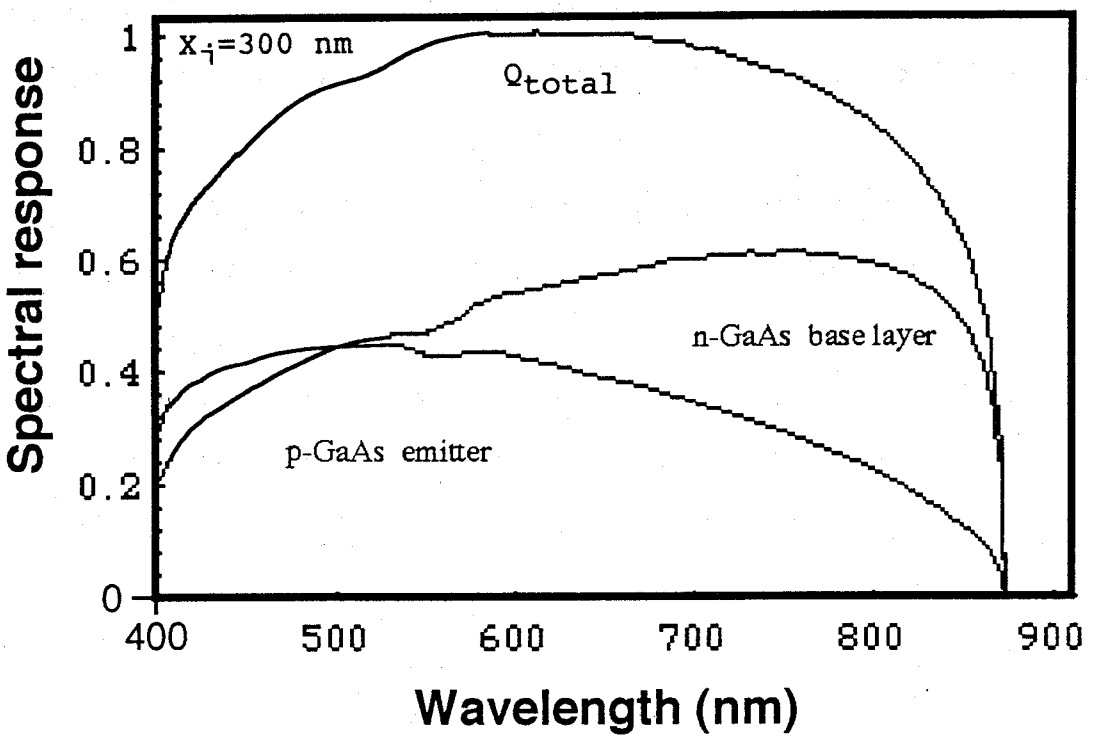


(a)

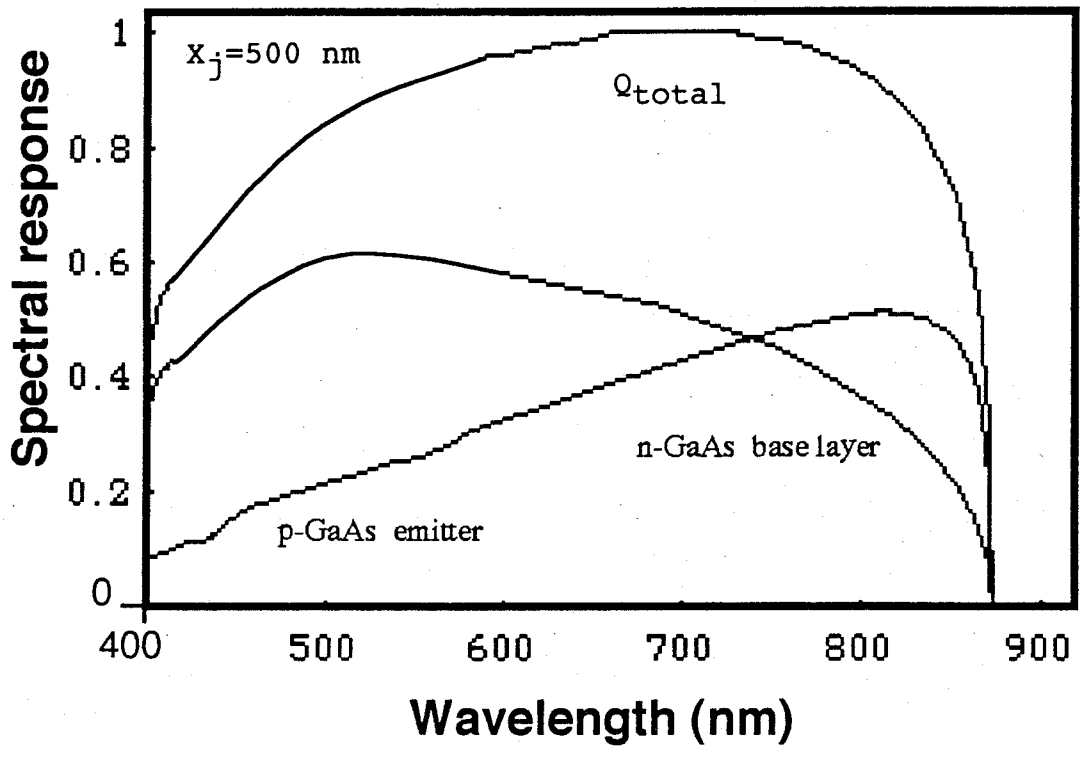


(b)

**Fig. 2-11 The influence of the junction depth Xj on the spectral response of the GaAs top cell on Si (under conditions: $N_A=3\times10^{18}$ $cm^{-3}$, $N_D=10^{16}$ $cm^{-3}$, $S_f=10^4$ cm/sec, $Nd=10^6$ $cm^{-3}$, E=0).**

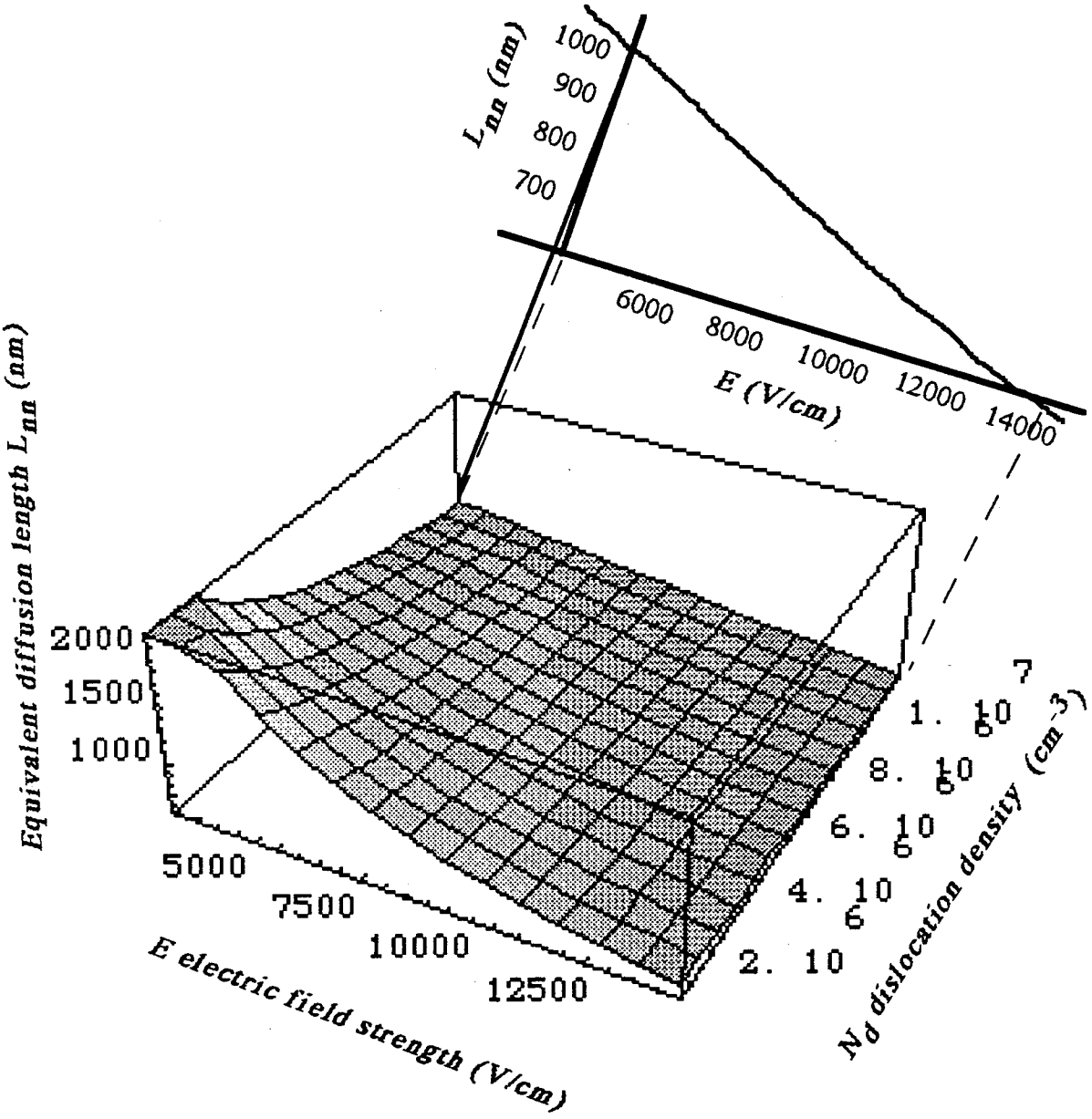


Fig. 2-12 The relationship of the equivalent diffusion length $L_{nn}$ vs. the dislocation density and the doping concentration when there is a electric field E in the p-GaAs emitter layer ($N_A=3\times10^{18}$ $cm^{-3}$).

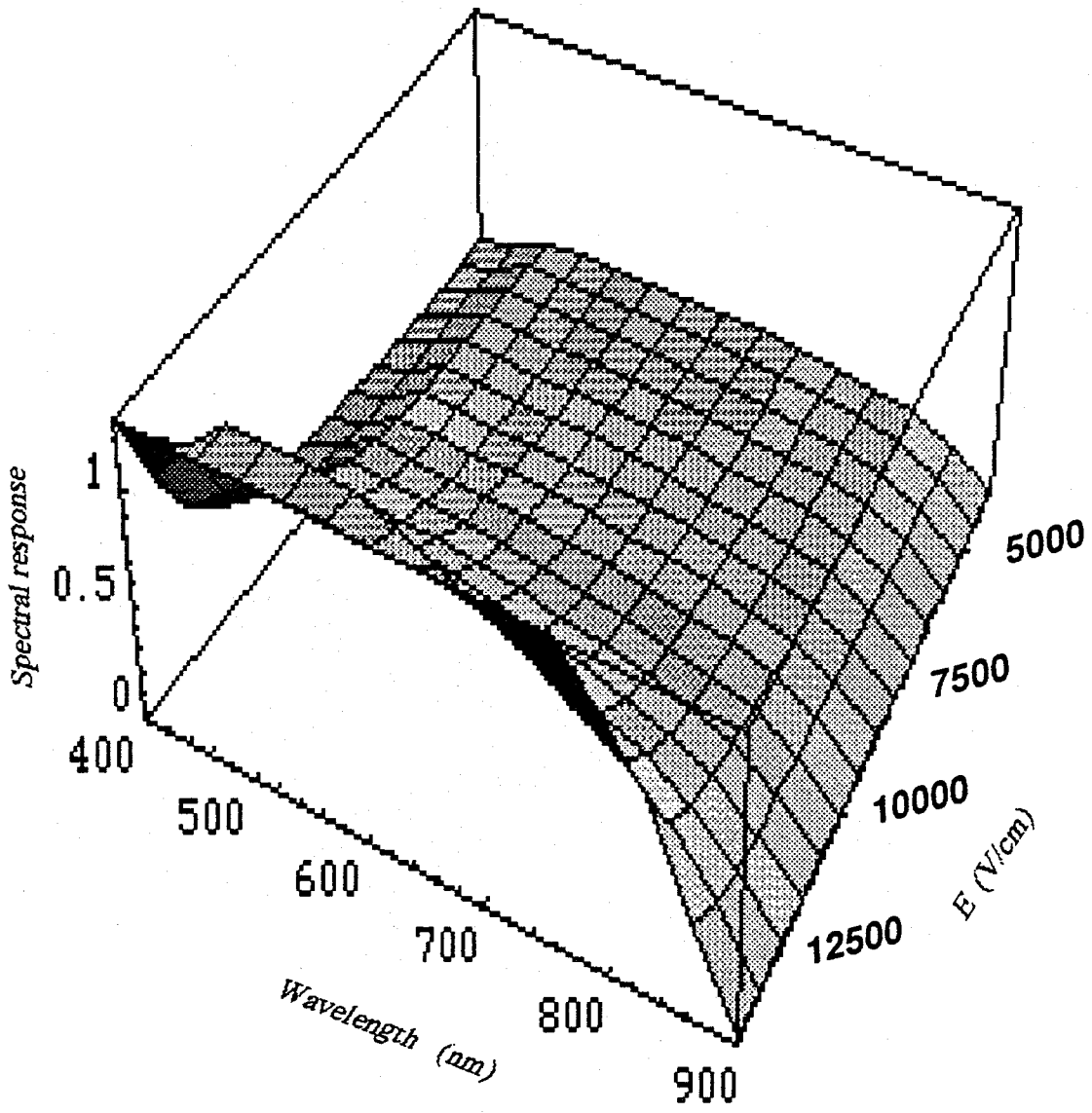


Fig. 2-13 Dependence of the spectral response of the GaAs cell on the electric field strength E in the p-GaAs emitter layer ($N_A=3\times10^{18}$ $cm^{-3}$, $N_D=1\times10^{16}$ $cm^{-3}$, $S_f=10^4$, $x_j=300$ nm, $N_d=10^4$ $cm^{-2}$).

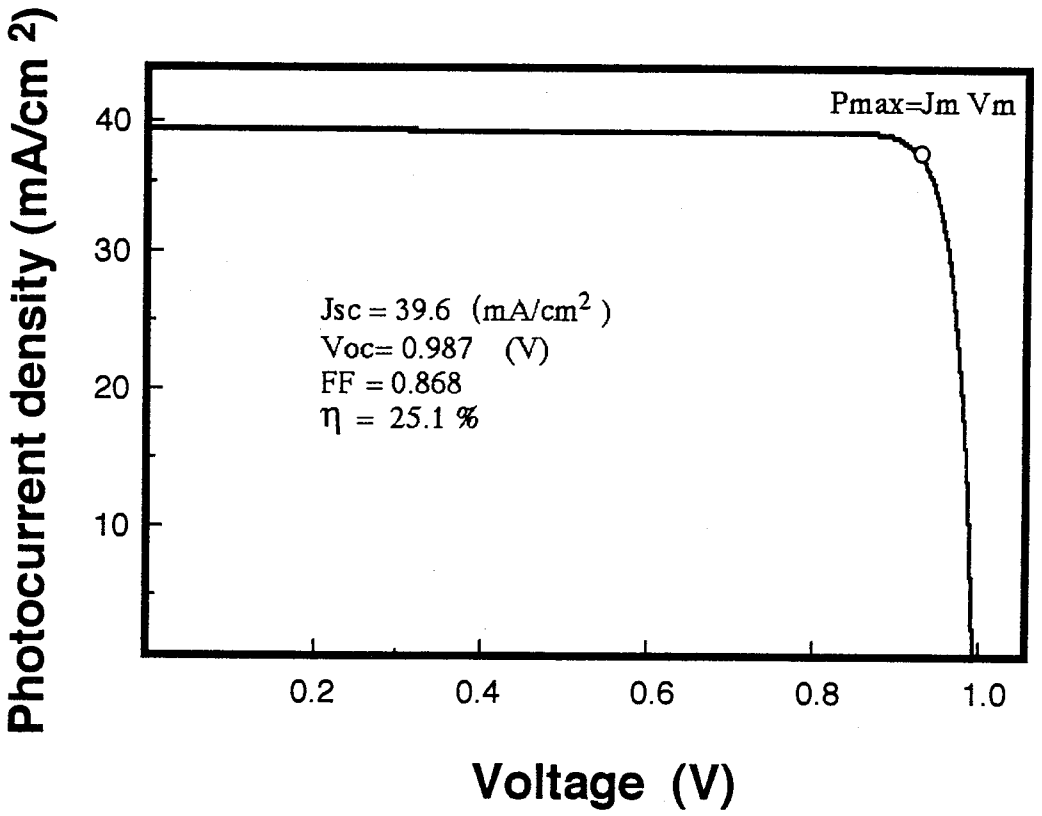


**Fig.2-14 Calculated AM0 conversion efficiency for the GaAs top cell with the structure parameters: a p-GaAs layer carrier concentration of $3\times10^{18}$ $cm^{-3}$, a junction depth of 0.3μm, an n-GaAs layer concentration of $1\times10^{16}$ $cm^{-3}$, the electric field strength of 14500 V/cm and the dislocation density of $10^4$ $cm^{-2}$.**

response of the GaAs top cell in a 3-dimensional graph vs. the electric field strength E. These results suggested that the spectral response of the GaAs top cell in the short wavelength region behaves almost perfect performance when the field strength is increased to 14500 V/cm. Fig. 2-14 shows the calculated current-voltage characteristics of the GaAs top cell with optimal parameters. The calculated AM0 conversion efficiency is 25.1%.

Fig. 2-15 shows the photocurrent density distribution of Si solar cell without (a) and with (b) a 3-μm-thick GaAs top cell on it. The total photocurrent ($J_{ph}$) consists of emitter layer current $J_p$, depletion layer current $J_{dr}$ and base layer current $J_n$. $J_n$ is the main quantity among them. There is a 3-μm-thick GaAs top cell on the Si cell and the incident light is almost completely absorbed in the wavelength region below the energy bandgap of GaAs. The total current $J_{ph}$ is dominated by the base layer current $J_n$ as shown in Fig.2-15 (b).

Fig. 2-16 shows the spectral responses of the Si bottom cell with various resistivities of Si substrate. The quantum efficiency increases with resistivity but when resistivity is up to 100 Ω·cm, the quantum efficiency is degraded because of the recombination at the rear surface.

Calculated AM0 conversion efficiencies of the Si bottom cell under 3-μm GaAs vs. the doping concentration of the p-Si base layer are shown in Fig. 2-17. Considering the effect of recombination at the rear surface, equation (2-24), the highest calculated efficiency of the Si bottom cell is 6.5% (Jsc=16.8 mA/cm$^2$, Voc=0.628, FF=0.833) with the the base layer

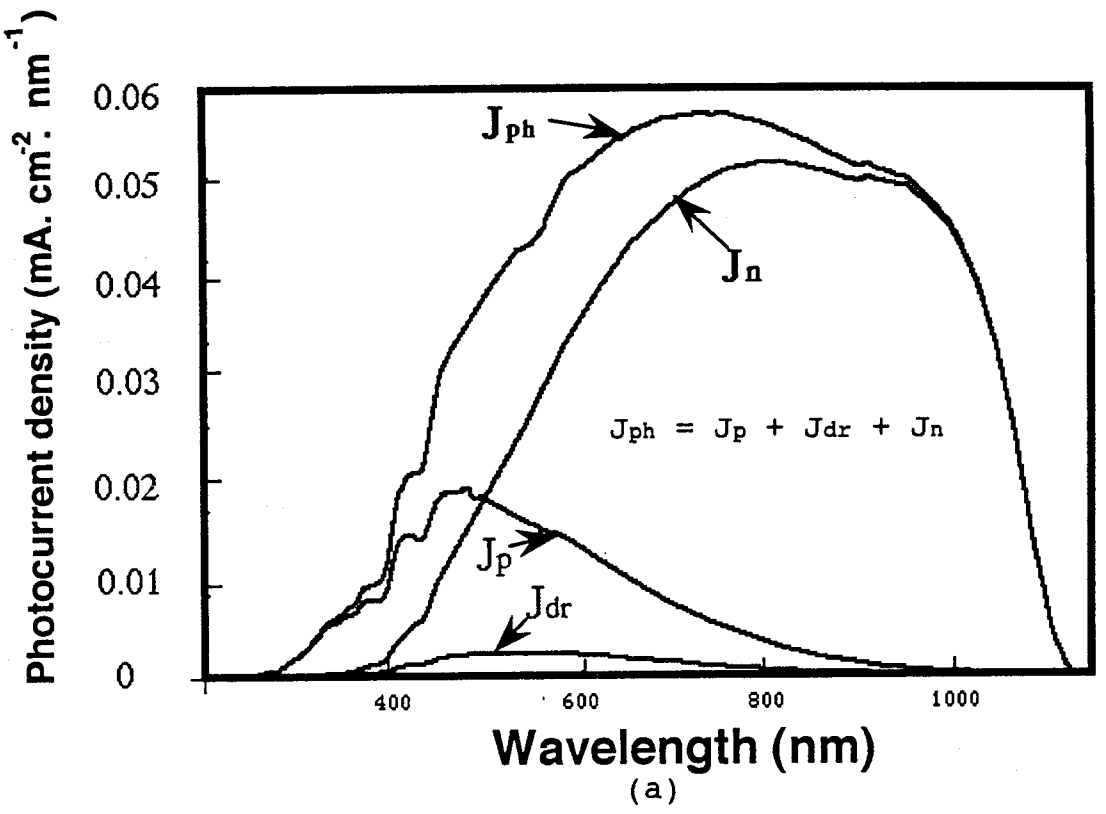


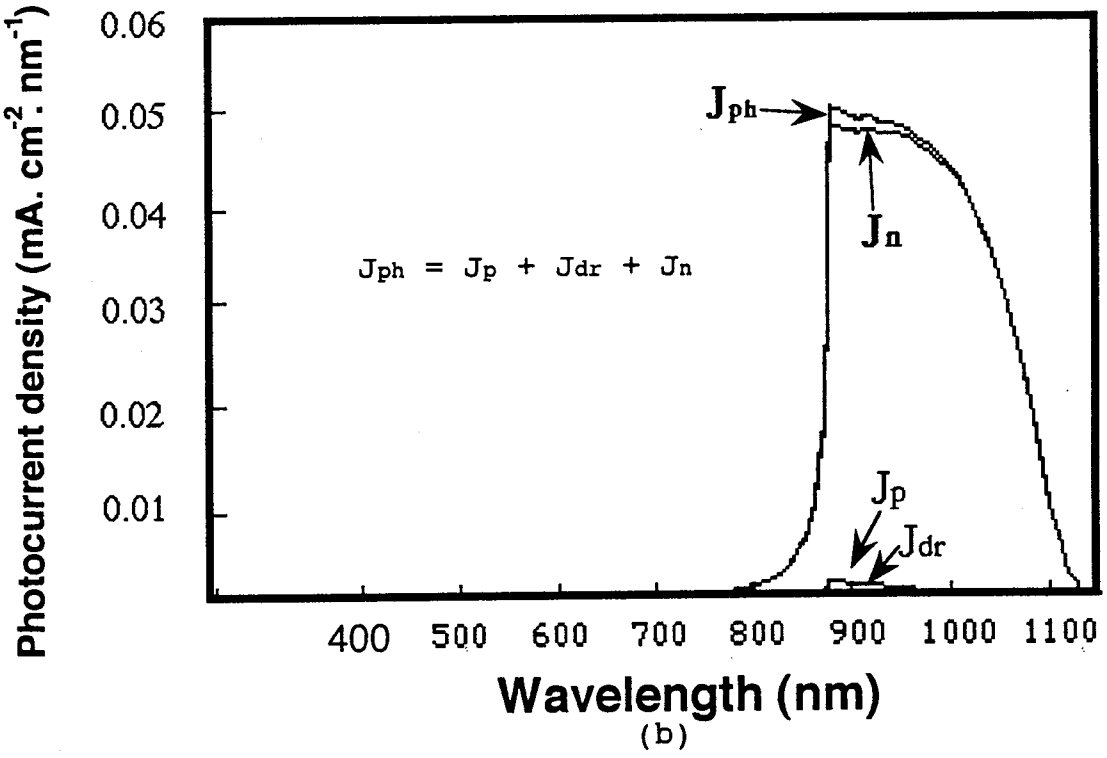


**Fig. 2-15 The photocurrent density distribution of Si solar cell vs wavelength without (a) and with (b) the 3μm-thick GaAs top cell on it.**

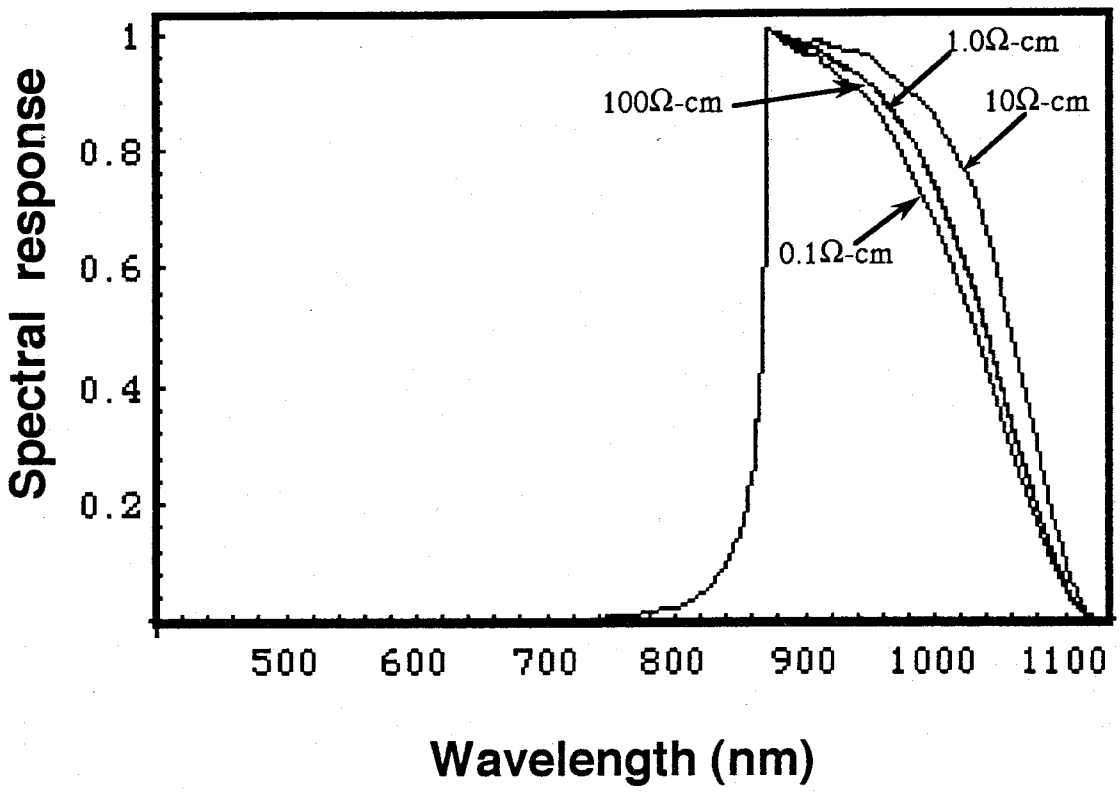


**Fig. 2-16 The variation of spectral response of the Si bottom cell with the doping concentration of p-Si base layer under the 3 μm-thick GaAs top cell.**

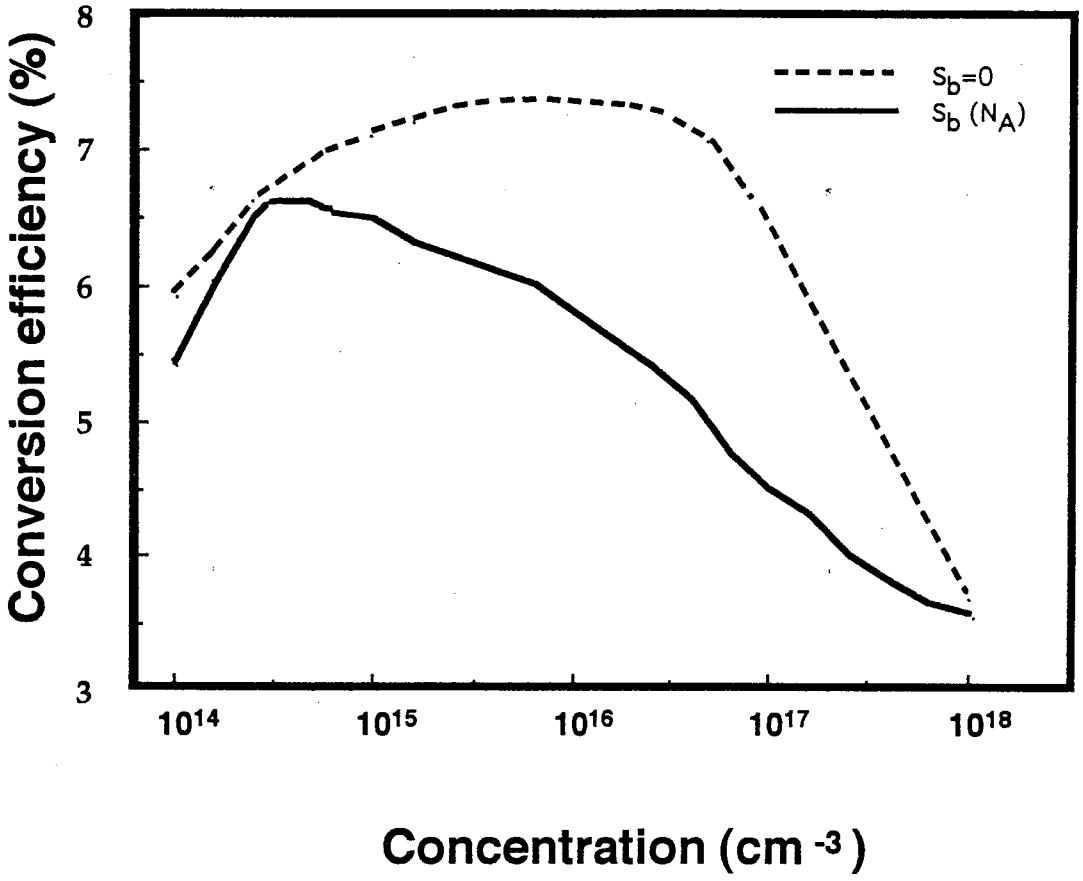


**Fig.2-17 Calculated AM0 conversion efficiency of the Si bottom cellunder the 3-μm-thick GaAs top cell vs. the doping concenctraion of p-Si base layer relative to the back surface recombination volecity, $S_b$.**

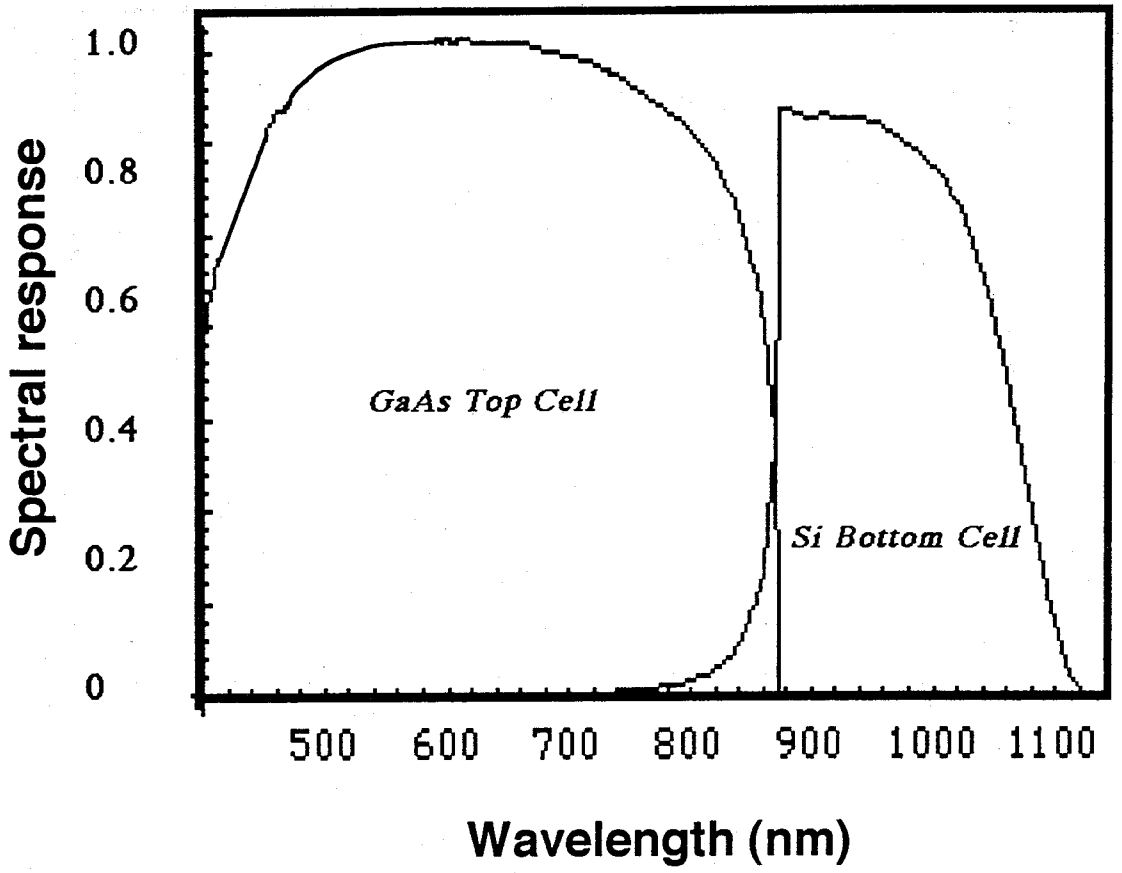


**Fig. 2-18 Calculated spectral response of the three-terminal GaAs/Si tandem solar cell.**

concentration of $6\times 10^{14}$ $cm^{-3}$. If $S_b$ =0, the calculated efficiency will be more than 7% in the region of the p-Si base layer concentration from $4\times10^{15}$ $cm^{-3}$ to $5\times10^{16}$ $cm^{-3}$.

Fig. 2-18 shows the calculated AM0 spectral response of the GaAs/Si three-terminal tandem solar cell with the optimal parameters. Combing the efficiencies of the GaAs top cell and the Si bottom cell, the total calculated efficiency of the GaAs/Si tandem cell is 31.6% under 1sun, AM0 conditions. The current-voltage characteristics are shown in Table 2-3.

**Table 2-3**
**Photovoltaic properties of the GaAs/Si three-terminal tandem solar cell (η: calculated AM0 efficiency).**

| Cell | Jsc ($mA/cm^2$) | Voc (V) | FF (%) | η (%) |
|---|---|---|---|---|
| GaAs top cell | 39.6 | 0.987 | 86.8 | 25.1 |
| Si bottom cell | 16.8 | 0.628 | 83.3 | 6.50 |
| GaAs/Si tandem cell | | | | **31.6** |

2-3-3. Two-termianl tandem soalr cell

Fig. 2-19 shows calculated spectral response of $Al_xGa_{1-x}As/Si$ ($x\sim0.22$) tandem solar cell vs. Al composition (x) of $Al_xGa_{1-x}As$ with 3-dimensional configuration. With increasing the Al content, the absorption-edge of the AlGaAs top cell shifts to the short wavelength region and the spectral response of the Si bottom cell becomes wider simultaneously.

For two-terminal configuration, it is necessary to demand the photocurrent matching condition between the top cell and the bottom cell in the optimal operation. Fig. 2-20 shows varieties of normalized short-circuit currents (Jsc) of the AlGaAs top cell and Si bottom cell with Al content of the $Al_xGa_{1-x}As$ top cell. Jsc of the AlGaAs top cell decreases and that of the Si bottom cell increases with Al composition. The photocurrent matching condition shall be satisfied at x=0.21 and the short-circuit currents of the top cell and the bottome cell have same value at Jsc=30 $mA/cm^2$. The I-V data are shown in Table 2-4.

**Table 2-4**
**Photovoltaic properties of the $Al_{0.21}Ga_{0.79}As/Si$ two-terminal tandem solar cell ($\eta$: calculated AM0 efficiency).**

| Cell | Jsc ($mA/cm^2$) | Voc (V) | FF (%) | $\eta$ (%) |
|---|---|---|---|---|
| Top cell | 29.9 | 1.12 | 87.5 | 21.7 |
| Bottom cell | 30.0 | 0.621 | 82.0 | 11.3 |
| Tandem cell | 29.9 | 1.74 | 84.0 | **32.3** |

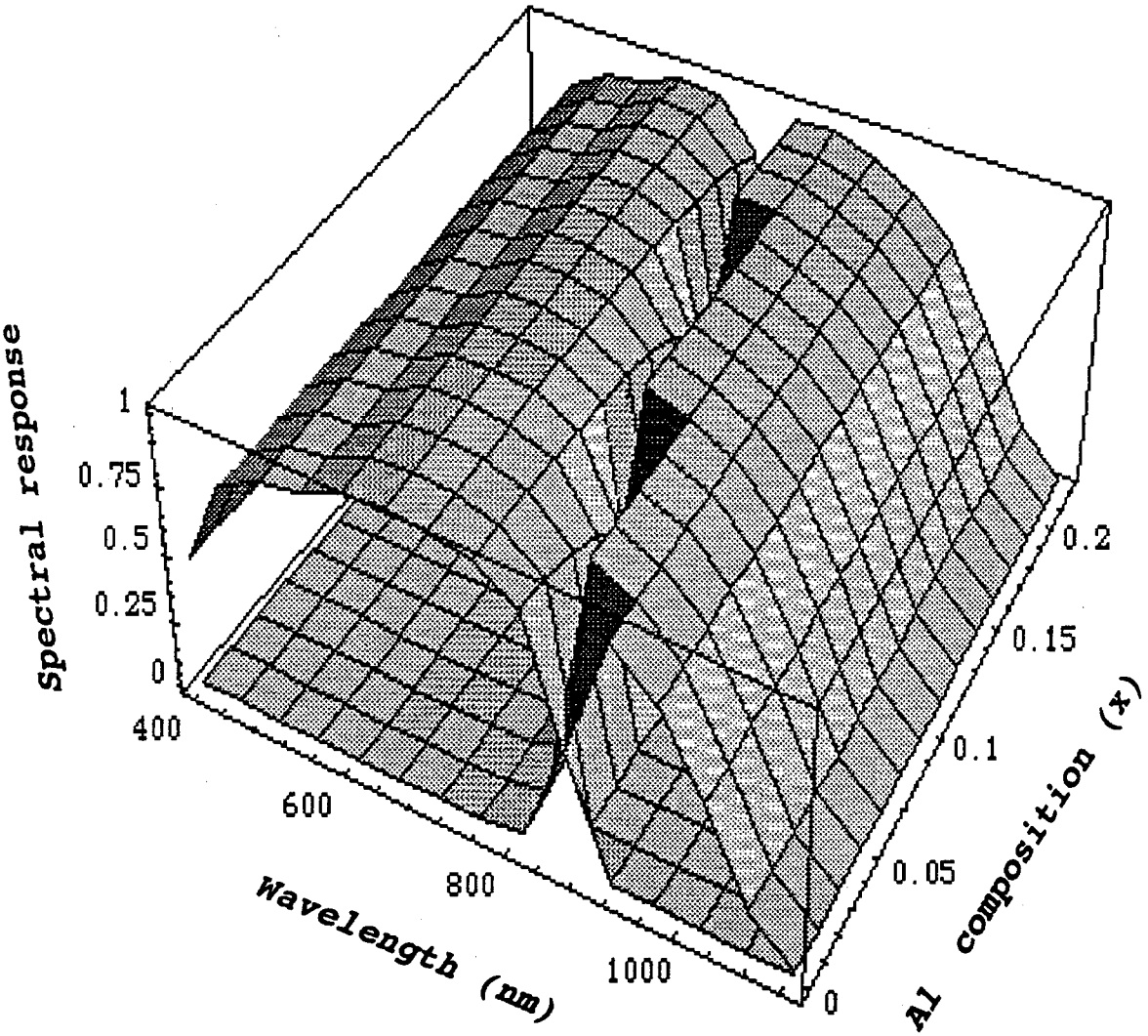


Fig.2-19 Calculated quantum efficiencies of $Al_xGa_{1-x}As/Si$ (x=0～0.22) two-terminal tandem solar cells vs. Al composition (x)

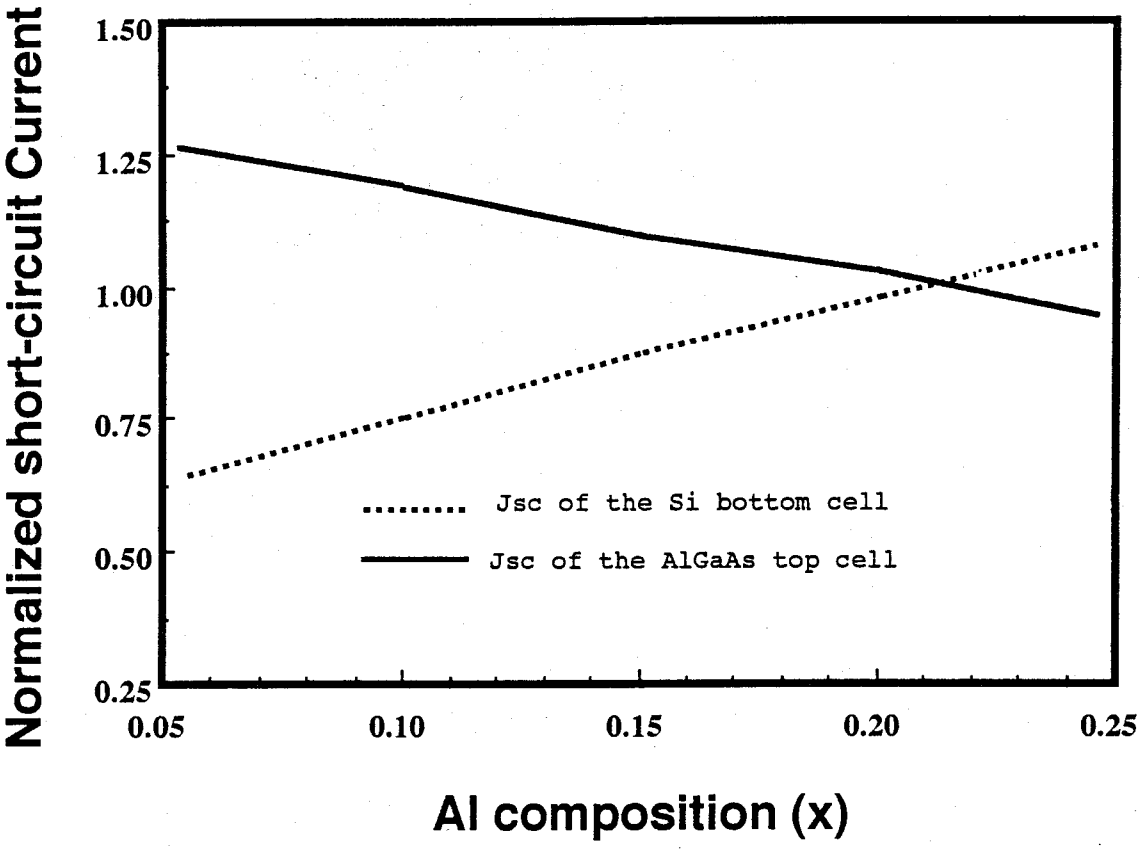


Fig.2-20 Calculated AM0 short-circuit currents of the AlGaAs top cell and the Si bottom cell with normalized values vs. the Al composition, x of the $Al_xGa_{1-x}As$ top cell.

## 2-4. Conclusion

In this Chapter, the material properties and the parameters of GaAs, AlGaAs, Si and GaAs-on-Si were reviewed in general, and the empirical expressions used in the calculation were described in detail. The theoretical calculation and design for high efficiency $Al_xGa_{1-x}As$/Si tandem solar cells were carried out. The structure design and the parameter optimization are concentrated on GaAs/Si three-terminal tandem solar cells and AlGaAs/Si two-terminal tandem solar cells, respectively. The calculations are based on the assumption that the reflection of solar cells is zero and AlGaAs window layer has no photo-absorption losses.

For GaAs/Si three-terminal tandem solar cells, the minority-carrier parameters used in the calculation are considered as the functions of the dislocations and the doping concentrations. Effects of the dislocation density ($N_d$) in GaAs-on-Si, the base layer doping concentration ($N_D$), junction depth ($X_j$), electric field strength (E) in the emitter layer on photovoltaic properties of the GaAs top cell were analyzed. From these results, it has been demonstrated that the AM0 efficiency of the GaAs top cell on Si about 25% can be expected by reducing the dislocation density below $1\times10^5$ $cm^{-2}$, employing an n-GaAs base layer concentration about $1\times10^{16}$ $cm^{-3}$, using a shallow p-n junction depth about 300 nm and a graded bandgap emitter layer with the strong electric field ($E \geqq$ 14500 V/cm). It is important to improve the spectral response of the Si bottom cell in the long wavelength region. Reducing

the recombination velocity of back surface ($S_b$) by passivation, using a Si substrate with high resistivity (~50 Ω·cm) and BSF structure, the efficiency of the Si bottom cell will be more than 7%. So that, combing the efficiency of the top cell and the bottom cell, the conversion efficiency over 31% can be achieved in theory for GaAs/Si three-terminal tandem solar cell.

The performances of $Al_xGa_{1-x}As$/Si two-terminal tandem solar cells were analyzed from the point of the photocurrent matching between the top cell and the bottom cell, assuming that the AlGaAs-on-Si material quality is good as AlGaAs-on-GaAs. When Al composition is about 0.21, the photocurrent matching between the top cell and the bottom cell could be satisfied (Jsc=30 mA/cm$^2$) and the conversion efficiency (1sun, AM0) of 32.3% could be obtained in theory.

References


1) M. P. Thekaekara: *Suppl. Proc. 20th Annu. Meet. Inst. Eviron. Sci.*, (1974) 21.

2) D. Trivich and P. A. Flinn: Solar Energy Research, (University of Wisconsin Press, Madison, 1955) p.143.

3) C. Amano, H. Sugiura, A. Yamamoto and M. Yamaguchi: Appl. Phys. Lett. **51** (1987) 1998.

4) T.Nishioka, Y. Itoh, N. Uchida, A. Yamamoto and M. Yamaguchi: *Technical Digest of the International PVSEV-3* (Tokyo, Japan, 1985) p.545.

5) M. F. Piszczor, D. J. Brinker, D. J. Flood, J. E. Avery, L. M. Fraas, E. S. Fairbanks and M. J. O'Neil: *Proceeding of the 22nd IEEE photovoltaic Spec. Conf.* (Las Vegas, USA, 1991) p.1458.

6) B. J. Stanbery, B. D. King, R. M. Murgess, R. W. McClelland, N. P. Kim, R. P. Gale and R. A. Mickelsen: IEEE Trans. Electron Devices **ED-37** (1990) 438.

7) B-C. Chung, G. F. Virshup and J. C. Schultz: *Proceeding of the 21st IEEE photovoltaic Spec. Conf.* (Florida, USA, 1990) p.179.

8) J. M. Olson, S. R. Kurtz, A. E. Kibbler and P. Faine: *Proceeding of the 21st IEEE photovoltaic Spec. Conf.* (Florida, USA, 1990) p.24.

9) R. D. Deslattes, A. Henins, H. A. Bowman, R. M. Schoonover, C. L. Carroll, I. A. Machlan, L. J. Moore and W. R. Shields: Phys. Rev. Lett. **33** (1974) 463.

10) E. G. Kessler, Jr, R. D. Deslattes and A. Henins: Phys. Rev. **A**, Vol.**19**, (1979) 215.

11) P. T. Barnett and T. F. Page: J. Mater. Sci. **20** (1985) 4624.

12) Y. Okada and Y. Tokumaru: J. Appl. Phys. **56** (1984) 314.

13) C. J. Glassbrenner and G. A. Slack: Phys. Rev. **134** (1964) **A**1058.

14) W. L. Kennedy, P. H. Sidies, G. C. Danielson: Adv. Energy Convers. **2** (1962) 53.

15) Y. P. Varshnic: Physica **A** (Netherlands) **34** (1967) 149.

16) D. E. Aspnes and A. A. Studna: Phys. Rev. **B 27** (1983) 985.

17) H. R. Philipp: J. Appl. Phys. **43** (1972) 2835.

18) E. A. Taft: J. Electrochem. Soc. **125** (1978) 968.

19) E. O. Filatova, A. S. Vinogradov, I. A. Sorokin and T. M. Zimkina: Sov. Phys.-Solid State **25** (1983) 736.

20) M. Morohashi, N. Sawaki and I. Akasaki: Jpn. J. Appl. Phys. Part 1, **24** (1985) 661.

21) A. Skumanich, D. Fournier and A. C. Boccara, N. M. Amer: Appl Phys, Latt. **47** (1985) 402.

22) A. Neugroschel: IEEE Electron. Device Lett. **EDL-6** (1985) 425.

23) M. C. Carotta, M. Merli, L. Passari and E. Susi: Appl. Phys. Lett. **49** (1986) 44.

24) S. E. Swirhun, Y.-H. Kark and R. M. Swanson: *Proc. Int. Electron Device Meeting,* (Los Angeles, USA, 1986) p.24.

25) V. G. Weizer and R. Delombard: Appl. Phys. Lett. **49** (1986) 201.

26) M. J. Chen and C. Y. Wu: Solid State Electron, **28** (1985) 751.

27) P. Lauwers, J. Van Meerberger, P. Bulted, R. Mertens and R. Van Overstraeten: Solid State Electron, **21** (1978) 747.

28) L. Passari and E. Susi: J. Appl. Phys. **54** (1983) 3935.

29) S. E. Swirhun, Y. H. Kwark and R. M. Swanson: *IEDM Tech. Dig.* (1986) 24.

30) M. Morohashi, N. Sawaki, T. Somatani and I. Akasaki: Jpn. J. Appl. Phys. Part 1, **22** (1983) 276.

31) J. A. del Alamo, S. Swirhun and R. M. Swanson: Proc. *Int. Electron Devices Meeting* (Washington, USA, 1985) p.290.

32) S. E. Swirhun, J. A. del Alamo and R. M. Swanson: IEEE Electron Device Lett. **EDL-7** (1986) 168.

33) D. Hunber, A. Bachmeier, R. Wahlich and H. Herzer: *Proc. Conf. Semiconductor Silicon* (Electrochemical Society, USA, 1986) p.1022.

34) C. H. Wang, K. Misiakos and A. Neugroschel: IEEE Transaction on Electron Devies **ED-37** (1990) 1314.

35) B. A. Boby and A. F. Kravchenko: Soc. Phys.-Acoustics **13** (1967) 242.

36) N. G. Kolin, et al : Phys. Chem. Mater. Treat. **21** (1987) 223.

37) L. Bernstin and R. J. Beales: J. Appl. Phys. **32** (1961) 122.

38) C. M. Bhandari and D. M. Rowe: *Thermal Conduction in Semiconductors* (Wiley, New York, 1988).

39) E. D. Palik: *Handbook of Optical Constants of Solid* (Academic press, New York, USA, 1985) p429.

40) W. Cohran, S. J. Fray, F. A. Quarrington and W. Williams: J. Appl. Phys. **34** (1961) 2102.

41) A. N. Pikhtin and A. D. Yas'kov: Sov. Phys.-Simecond. **12** (1978) 622.

42) Y. P.Varshni: Physica **34** (1967) 149.

43) N. G. Ainslie, S. E. Blum and J. F. Woods: J. Appl. Phys. **33** (1962) 2391.

44) M. I. Nathan, W. P. Dumke, K. Wrenner, S. Tiwari, S. L. Wright and K. A. Jenkins: Appl. Phys. Lett. **52** (1988) 654.

45) H. Ito and T. Ishibashi: J. Appl. Phys. **65** (1989) 5197.

46) K. L. Ashley and J. R. Biard: IEEE Trans. Electron Devices, **ED-14** (1967) 429.

47) J. S. Blakemore: J. Appl. Phys. **53** (1982) R123.

48) R. J. Nelson and R. G. Sobers: J. Appl. Phys. **49** (1978) 6103.

49) E. Yablonovitch, R. Bhat, J. P. Harbison and R. A. Logan: Appl. Phys. lett. **50** (1987) 1197.

50) S. A. Ringel and A. Rohatgi: *Proceeding of the 20th IEEE photovoltaic Spec. Conf.* (USA, 1988) p.666.

51) W. Shockley and H. J. Queisser: J. Appl. Phys. **32** (1961) 510.

52) S. Adachi: J. Appl. Phys. **53** (1982) 5863.

53) S. Adachi: J. Appl. Phys. **53** (1982) 8775.

54) S. Adachi: J. Appl. Phys. **54** (1983) 1844.

55) S. Adachi and K. Oe: J. Appl. Phys. **54** (1983) 6620.

56) S. Adachi and K. Oe: J. Appl. Phys. **56** (1984) 74.

57) S. Adachi and K. Oe: J. Appl. Phys. **56** (1984) 1499.

58) M. Ilegems: *The Technology and Physics of Molecular Beam Epitaxy* (Plenum Publishing Corporation, London, 1985).

59) A. K. Saxena: J. Inst. Electron. Telecommun. Eng. **29** (1985) 97.

60) A. K. Saxena and M. A. L. Mudares: J. Appl. Phys. **58** (1985) 2795.

61) K. Masu, E. Tokumitsu, M. Konagai and K. Takahashi: J. Appl. Phys. **54** (1983) 5785.

62) G. W.'t Hooft, C. van Opdorp. H. Veenliet and A. T. Vink: J. Crystal Growth, **55** (1981) 173.

63) R. H. Wllis, M.-AdiForte Poisson, M. Bonnet and G. Beuchet: Int. Phys. Conf. Ser. **56** (1981) 73.

64) R. J. Nelson and R. G. Sobers: J. Appl. Phys. **49** (1978) 6103.

65) J. M. Olson, S. R. Kurtz, A. E. Kibbler and P. Paine: Appl. Phys. Lett. **55** (1989) 1741.

66) M. Umeno, Y. Azuma, T. Egawa, T. Soga and T. Jimbo: *Proceeding of the 23rd IEEE photovoltaic Spec. Conf.* (Louisville, USA, 1993) p.741.

67) M. Yang, T. Soga, T. Jimbo and Umeno: Solar Energy and Solar Cells, **35** (1994) 45.

68) S. N. G. Chu, S. Nakahara, S. J. Pearton, T. Boone and S. M. Vernon: J. Appl. Phys. **64** (1988) 2981.

69) N. Chand, F. Ren, A. T. Marrander, J. P. van der Ziel, A. M. Sergent, R. Hull, S. N. Chu, Y. K. Chen and P. V. Lang: J. Appl. Phys. **67** (1990) 2343.

70) S. Sakai: Appl. Phys. Lett. **51** (1987) 1069.

71) W. Stoltz, F. E. G. Guimaraes and K. Ploog: J. Appl. Phys. **63** (1988) 492.

72) N. Chand, R. People, F. A. Baiocchi, K. W. Wecht and A.

Y.Cho: Appl. Phys. Lett. **49** (1986) 815.

73) J. P. van der Ziel, N. Chand and J. S. Weiner: J. Appl. Phys. **66** (1989) 1195.

74) B. G. Yacobi, C. Yagannath, S. Zemon and P. Sheldon: Appl. Phys. Lett. **52** (1988) 555.

75) S. Zemon, C. Jagannath, S. K. Shastry and G. Lambert: Solid State Commun. **65** (1988) 553.

76) N. Hayafuji, S. Ochi, M. Miyashita, M. Tsugami, T. Murotani and A. Kawagishi: J. Crystal Growth **93** (1988) 494.

77) T. Soga, T. Jimbo and M. Umeno: Jpn. J. Appl. Phys. **33** (1994) 1494.

78) R. K. Ahrenkiel, M. M. Al-Jassim, D. J. Dunlavy and K. M. Jones: Appl. Phys. Lett. **53** (1988) 222.

79) M. A. Green, A. W. Blakers, J. Zhao, A. M. Mile, A. Wang and X. Dai: IEEE Trans. Electron Dev. **ED-37** (1990) 331.

80) S. R. Kurtz, J. M. Olson and A. Kibbler:*Proceeding of the 21st IEEE photovoltaic Spec. Conf.* (Las Vegas, USA, 1991) p.138.

81) J. C. C. Fan, B-Y. Tsaur and B. J. Palm: *Proceeding of the 16th IEEE photovoltaic Spec. Conf.*(San Diego, USA, 1982) p.692.

82) H. J. Hovel: *Semiconductors and Semimetals*, Vol.11, Solar Cells (Academic press, New York, 1975)

83) S. M. Sze: *Physics of Semiconductor Devices* (A Wiley-Interscience publication. New York, USA, 1981) p.790.

84) M. Yamaguchi, C. Amano and Y. Itoh: J. Appl. Phys. **66** (1989) 915.

85) John C. Zolper and Allen M. Barnett: IEEE. Trans. Electron Devices **37** (1990) 478.

86) M. Yamaguchi and C. Amano: J. Appl. Phys. **58** (1985) 3601.

87) A. Aberle, W. Werta, J. Knobloch and B. Vob: *Proceeding of the 21st IEEE photovoltaic Spec. Conf.* (Florida, USA, 1990) p.233.

88) A. A. Immorlica, Jr. and G. L. Pearson: Appl. Phys, Lett. **25** (1974) 570.

89) M. P. Thekaekara: Solar Energy, **14** (1973) 109.